

# AN EFFICIENT METHOD FOR SOLVING ELECTROSTATIC PROBLEMS

*The boundary element method is a widely used numerical technique, but for problems with singularity caused by a degenerate boundary, the coincidence of the boundaries gives rise to a difficult problem that requires a troublesome subdomain technique. The dual boundary element method provides fast, accurate, and efficient solutions.*

**E**lectrostatic problems are those that deal with the effects of electric charges at rest. For modern electron and micro-electromechanical systems (MEMS), an accurate electrostatic analysis is both essential and indispensable. We know that if we use the conventional boundary element method (BEM) for electrostatic problems that have singularity due to degenerate boundaries, the coincidence of the boundaries gives rise to a difficult, or ill-conditioned, problem. The coincidence is when different elements use the same nodes, but there is a free-edge between the elements.

In a degenerate boundary problem, the spatial coincidence of the two sides of the degenerate boundary leads to the singular integral equation on one side being indistinguishable from that on the other, even though the potentials on the two sides differ.<sup>1</sup>

Our dual boundary element method (DBEM)

uses a dual integral formulation with a hypersingular integral to solve boundary value problems in which singularity arises from degenerate boundaries. To prove this, we analyzed an electrostatic problem to check the mathematical model's validity; the analysis also showed that we could avoid deploying artificial boundaries and encountering the ill-conditioned problem of the conventional BEM and still get a more accurate and reasonable result.

In this article, we compare results between finite-element method (FEM) and DBEM analyses to prove the DBEM's superiority. Because model creation requires the most effort in electrical engineering practices, we strongly recommend the DBEM for industrial applications.

## Diverse Numerical Techniques

Numerical solution of electrostatic and electromagnetic (EM) problems<sup>2</sup> started in the mid 1960s with the introduction of high-speed digital computers. Since then, researchers have expended considerable effort on solving practical, complex EM-related problems for which closed-form analytical solutions are either intractable or not available. Numerical approaches let untrained users solve problems without knowledge of higher mathematics or physics, resulting in an

1521-9615/03/\$17.00 © 2003 IEEE  
Copublished by the IEEE CS and the AIP

SHIANG-WOEI CHYUAN AND YUNN-SHIUAN LIAO

*National Taiwan University*

JENG-TZONG CHEN

*National Taiwan Ocean University*

economy of labor on the part of the highly trained personnel.

Among different numerical approaches, the FEM and BEM (thanks to increasing developments in digital computer power) have moved from being tools for select research groups to powerful design tools for a broad class of engineers. The FEM is one of the most widely used numerical techniques because it can model extremely complex configurations and easily determine the response at any desired point of a structure, but the BEM has a few advantages over it. For example, it's easy to mesh and apply adaptive error control techniques to apply to it, and its efficiency is much higher than the FEM's when facing an infinite field.

### Degenerate Boundaries and the BEM

Although the BEM has become a widely accepted tool for solving engineering problems<sup>3</sup>—easy data preparation due to one-dimension reduction makes it attractive for practical use—a potential disadvantage of using it is poor analysis efficiency. BEM formulations generate dense matrices. For matrix operation and computation, solving sparse (symmetric) matrices of the FEM is easier and more accurate than solving the BEM's dense (asymmetric) matrices.

Using the subdomain technique in the BEM with artificial boundaries for the degenerate boundary ensures a unique solution. (In the subdomain technique, if we divide the concerned domain into different subdomains using the conventional BEM, new interfaces form between the subdomains. This introduces unknowns in the artificial boundary, so new constraints of the continuity and equilibrium conditions are necessary.) However, the technique's main drawback is that the deployment of artificial boundaries is arbitrary and thus cannot be implemented in an automatic procedure very easily. In addition, model creation is more troublesome than in the single-domain approach because there is no interface.

To tackle such degenerate boundary problems, Jeng-Tzong Chen and Hong-Ki Hong first proposed dual integral formulations in 1988.<sup>4</sup> Using the dual integral formulations, all boundary value problems can be well posed and solved efficiently in the original single domain. The Wessex Institute of Technology group first called this numerical implementation the dual boundary element method in 1992.<sup>5</sup>

### Comparing the DBEM to the BEM

Even for electrostatic problems without singularity arising from degenerate boundary, the DBEM has some advantages over conventional BEM.<sup>1</sup> One advantage is that an essential ingredient for all adaptive uses of the BEM is a reliable estimate of the local error. The hypersingular integral equation used in the DBEM is a complementary equation available for error estimation.

Another advantage is that we can use this hypersingular integral equation to calculate the tangent electric field directly instead of using the obtained potential field's numerical derivative. Researchers have formulated the tangent derivative along the boundary in terms of both the boundary potential and the boundary normal flux. Therefore, we could eliminate the numerical error from the BEM-facing side fringing—meaning, near the electron device's side boundary, the electric field will be distorted.

Finally, in the FEM and BEM, the stiffness matrix's symmetry requirement is especially useful. Because some researchers use the FEM and BEM to solve problems simultaneously, some coupled interfaces such as artificial boundaries form. The four kernel functions  $U(s,x)$ ,  $T(s,x)$ ,  $L(s,x)$ , and  $M(s,x)$  in the dual integral equations display the elegant structure of potential theory. We have found the symmetry and transpose symmetry properties for the DBEM's four kernel functions. Generally, the matrices of kernel functions used in the conventional BEM are asymmetric, and the matrices of kernel functions  $U(s,x)$ ,  $T(s,x)$ ,  $L(s,x)$ , and  $M(s,x)$  used in the DBEM are symmetric.

### The DBEM's Integral Formulation

The electrostatic problem essentially consists of finding the unknown potential function  $\Phi$  (or  $V$ ) of a partial differential equation. In addition to the fact that  $\Phi$  satisfies Laplace's equation within a prescribed solution region  $D$ ,  $\Phi$  must satisfy certain conditions on  $B$ , which is the boundary of  $D$ . Usually these boundary conditions are the Dirichlet ( $\Phi(x) = f(x)$ ) and Neumann ( $\partial\Phi(x)/\partial n_x = g(x)$ ) types. Therefore, we can write the governing equation (Equation 1) and boundary conditions (Equations 2 and 3) of electrostatic problems as follows:

$$\nabla^2 \Phi(x) = 0, \quad x \text{ in } D \quad (1)$$

$$\Phi(x) = f(x), \quad x \text{ on } B \quad (2)$$

**Table 1. The explicit forms of four kernel functions in dual integral equations.**

Kernel function	$U(s,x)$	$T(s,x)$	$L(s,x)$	$M(s,x)$
Order of singularity	Weak	Strong	Strong	Hypersingular
Two-dimensional case	$\ln(r)$	$-\gamma_i n_i / r^2$	$\gamma_i \bar{n}_i / r^2$	$2\gamma_i \gamma_j n_i \bar{n}_j / r^4 - n_i \bar{n}_i / r^2$
Three-dimensional case	$-1/r$	$-\gamma_i n_i / r^3$	$\gamma_i \bar{n}_i / r^3$	$3\gamma_i \gamma_j n_i \bar{n}_j / r^5 - n_i \bar{n}_i / r^3$
Remark	$r^2 = \gamma_i \gamma_j$	$n_i = n_i(s)$	$\bar{n}_i = n_i(x)$	$\gamma_i = x_i - s_i$

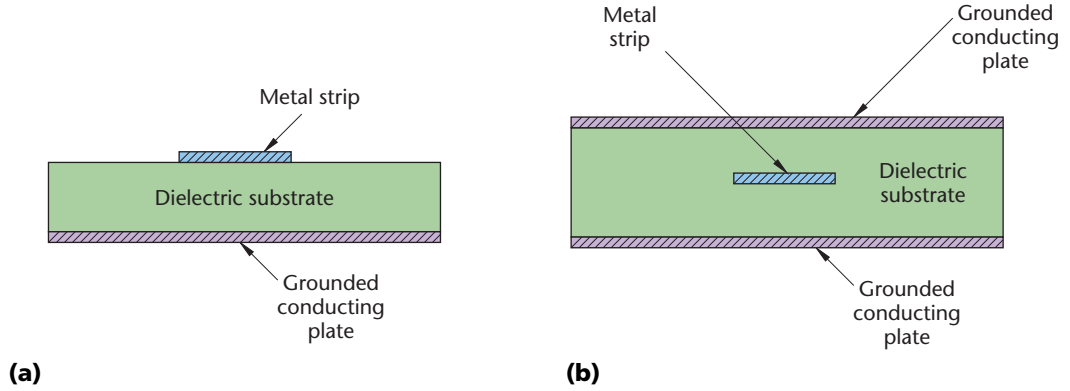


**Figure 1. Two types of microstrip lines: (a) stripline and (b) triplate line.**

$$\partial\Phi(x)/\partial n_x = g(x), \quad x \text{ on } B, \quad (3) \quad L(s,x) = \partial U(s,x)/\partial n_x, \quad (8)$$

where  $f(x)$  and  $g(x)$  denote known boundary data, and  $n_x$  is the unit outer normal vector at the point  $x$  on the boundary.

Using Green's identity, we can write the first equation of the dual boundary integral formulation for the domain point  $x$  as

$$2\pi\Phi(x) = \int_B T(s,x) \Phi(s) dB(s) - \int_B U(s,x) [\partial\Phi(s)/\partial n_s] dB(s) \quad (4)$$

for the two-dimensional case; for the three-dimensional case,  $4\pi$  must replace  $2\pi$ .

We devote the following derivations to the two-dimensional case for simplicity. After taking the normal derivative of Equation 4 with respect to the  $n_x$  direction, we can derive the second equation (hypersingular integral equation) of the dual boundary integral equations for the domain point  $x$ :

$$2\pi[\partial\Phi(x)/\partial n_x] = \int_B M(s,x) \Phi(s) dB(s) - \int_B L(s,x) [\partial\Phi(s)/\partial n_s] dB(s). \quad (5)$$

In Equations 4 and 5,

$$U(s,x) = \ln(r), \quad (6)$$

$$T(s,x) = \partial U(s,x)/\partial n_s, \quad (7)$$

and

$$M(s,x) = \partial^2 U(s,x)/\partial n_x \partial n_s, \quad (9)$$

where  $r = |s - x|$ ,  $s$  and  $x$  being position vectors of the points  $s$  and  $x$ , respectively, and  $n_s$  is the unit outer normal vector at point  $s$  on the boundary. In addition,  $U(s,x)$  is a fundamental solution,  $T(s,x)$  is the directional derivative in the  $n_s$  direction of  $U(s,x)$ ,  $L(s,x)$  is the directional derivative in the  $n_x$  direction of  $U(s,x)$ , and  $M(s,x)$  is the directional derivative in the  $n_x$  direction of  $T(s,x)$ .

Equations 4 and 5 together are termed the dual boundary integral formulation for the domain point. Table 1 shows the explicit forms of the four kernel functions  $U(s,x)$ ,  $T(s,x)$ ,  $L(s,x)$ , and  $M(s,x)$ . By tracing the domain point  $x$  to the boundary, we can derive the dual boundary integral equations for the boundary point  $x$ :

$$\alpha\Phi(x) = \text{CPV} \int_B T(s,x) \Phi(s) dB(s) - \text{RPV} \int_B U(s,x) [\partial\Phi(s)/\partial n_s] dB(s) \quad (10)$$

$$\alpha[\partial\Phi(x)/\partial n_x] = \text{HPV} \int_B M(s,x) \Phi(s) dB(s) - \text{CPV} \int_B L(s,x) [\partial\Phi(s)/\partial n_s] dB(s), \quad (11)$$

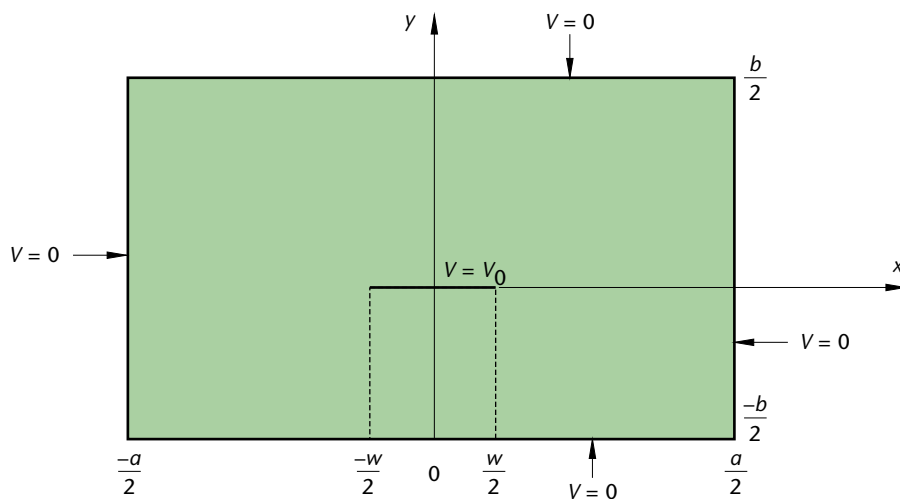


**Figure 2. Cross-section of strip transmission line.** For efficient point-to-point transmission of power and information, the source energy must be directed or guided. Parallel-plate transmission line is one of the most common types of guiding structures that support TEM waves. This type of transmission line consists of two parallel conducting plates separated by a dielectric slab of a uniform thickness.

where RPV is the conventional Riemann or Lebesgue integral, CPV is the Cauchy principal value, HPV is the Hadamard or Mangler principal value,<sup>2</sup> and  $\alpha$  depends on the collocation point ( $\alpha = 2\pi$  for an interior point,  $\alpha = \pi$  for a smooth boundary, and  $\alpha = 0$  for an exterior point). Equations 10 and 11 are called the dual boundary integral formulation for the boundary point—applying the normal derivative's operator to Equation 10 derives Equation 11.

### Solving Electrostatic Problems with Degenerate Boundaries How the DBEM Works

The development of solid-state microwaves and systems has led to the widespread use of a form of parallel-plate transmission lines called microstrip lines, or simply striplines. A stripline usually consists of a dielectric substrate sitting on a grounded conducting plane, with a thin narrow metal strip on top of the substrate (see Figure 1a).<sup>6</sup>

When the substrate has a high dielectric constant, a transverse electromagnetic (TEM) approximation is reasonably satisfactory. Electric field and magnetic field are perpendicular to each other, and both are transverse to the direction of propagation. It is a particular case of a TEM wave. Not all the fields will be confined in the dielectric substrate—some will stray from the top strip into the region outside the strip, causing interference in the neighboring circuits.

One method to reduce the stray field of striplines shown in Figure 1a is to have a grounded conducting plane on both sides of the dielectric substrate and to put the thin metal strip in the middle (see Figure 1b).<sup>6</sup> This arrangement is known as a triplate line. Because finding an exact analytical solution of the triplate line in Figure 1b that satisfies all boundary conditions is difficult, we can't accurately simulate the side-fringing effect. The thin metal strip appears as in Figure 1b, so a degenerate boundary is formed in the BEM simulation.

For nondegenerate boundary problems, we can use either the conventional BEM (the  $U(s,x)$  and  $T(s,x)$  kernels of Equations 6 and 7 or the  $L(s,x)$  and  $M(s,x)$  kernels of Equations 8 and 9) or the DBEM (using all four kernels). But for electrostatic problems with singularity from a degenerate boundary (like in Figure 1b), the DBEM plays an important and efficient role because we can't use the conventional BEM without artificial boundaries.

To check the model's validity, let's look at a simplified case study. Consider a strip conductor enclosed in a shielded box containing homogeneous medium (see Figure 2). If we assume the TEM propagation mode, our problem is reduced to finding  $V$  to satisfy Laplace's equation  $\nabla^2 V = 0$ . Let's determine the electric potential distribution inside the shielded box with the FEM and DBEM. Because obtaining analytical solutions via analytical methods is not easy, we used an FEM sim-

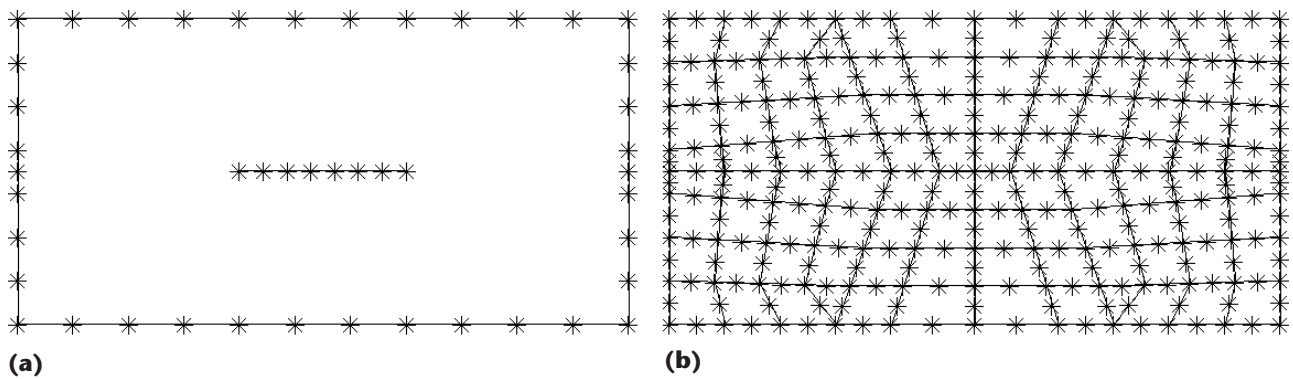


Figure 3. The (a) dual boundary element method (DBEM) mesh discretization of 52 elements and 46 nodes and the (b) finite-element method (FEM) mesh discretization of 96 elements and 321 nodes.

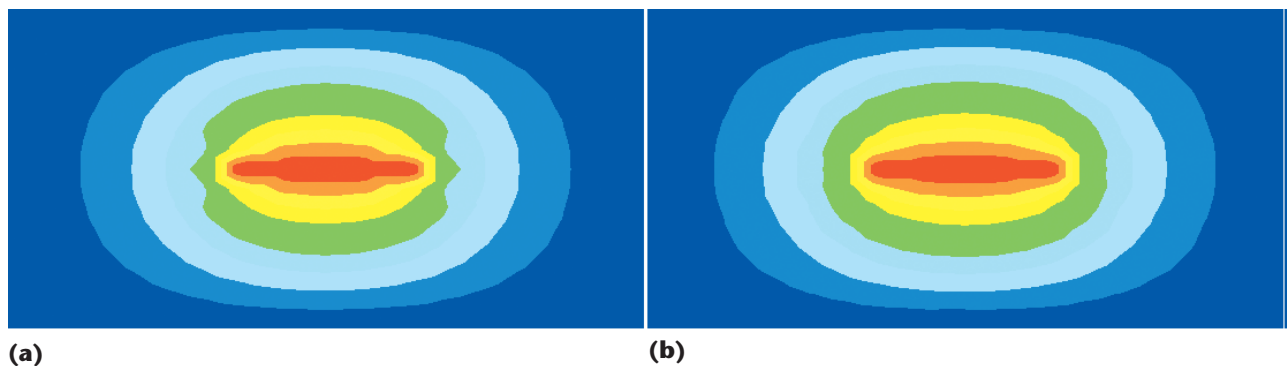


Figure 4. The results of the electric potential field (equipotential lines) using (a) the DBEM and (b) the FEM. The voltage value at the central area (red) is  $V_0$ ; near outside boundary (blue), it is zero.

Table 2. The results of electric potential under diverse numerical methods.

Locations ( $x, y$ )	Results from the conventional BEM $U, T$ kernels	Results from the direct BEM $L, M$ kernels	Results from the DBEM $U, T, L, M$ kernels	Results from the FEM	Difference between the DBEM and the FEM (%)
(10.000, 3.75)	N/A	N/A	0.70048 $V_0$	0.7104 $V_0$	-1.396
(11.558, 3.75)	N/A	N/A	0.66288 $V_0$	0.6742 $V_0$	-1.679
(12.338, 1.25)	N/A	N/A	0.17862 $V_0$	0.1863 $V_0$	-4.122
(-3.25, -5.62)	N/A	N/A	0.39078 $V_0$	0.4082 $V_0$	-4.268

ulation to compare with the DBEM.

To tackle such degenerate boundary problems, we used the dual integral formulations already presented in this article to solve the problem. For convenience, we assume the  $w$ ,  $a$ , and  $b$  values to be 5, 20, and 10, respectively. We analyze the four points using rough mesh discretization (52 elements and 46 nodes; see Figure 3a) of the DBEM, and then we compare the results with reference data computed from the

FEM (96 elements and 321 nodes; see Figure 3b). Table 2 lists the results of electric potential under diverse numerical methods; Figure 4 illustrates them. Comparing the results of the electric potential field (equipotential lines) using the DBEM (Figure 4a) and the FEM (Figure 4b), we see that the difference of electric potential distribution is small. Therefore, the DBEM used here is efficient.

Because the boundary condition in this case is

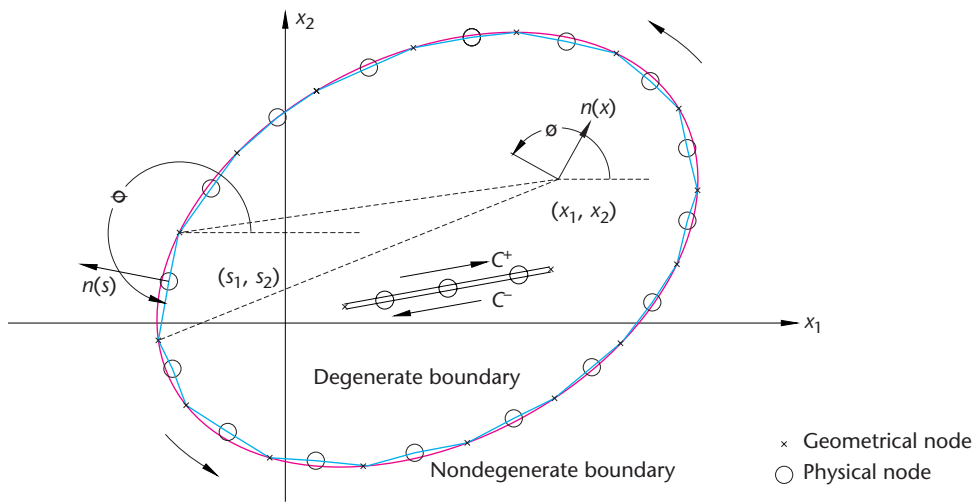


Figure 5. Boundary element discretization for the degenerate and nondegenerate boundaries.

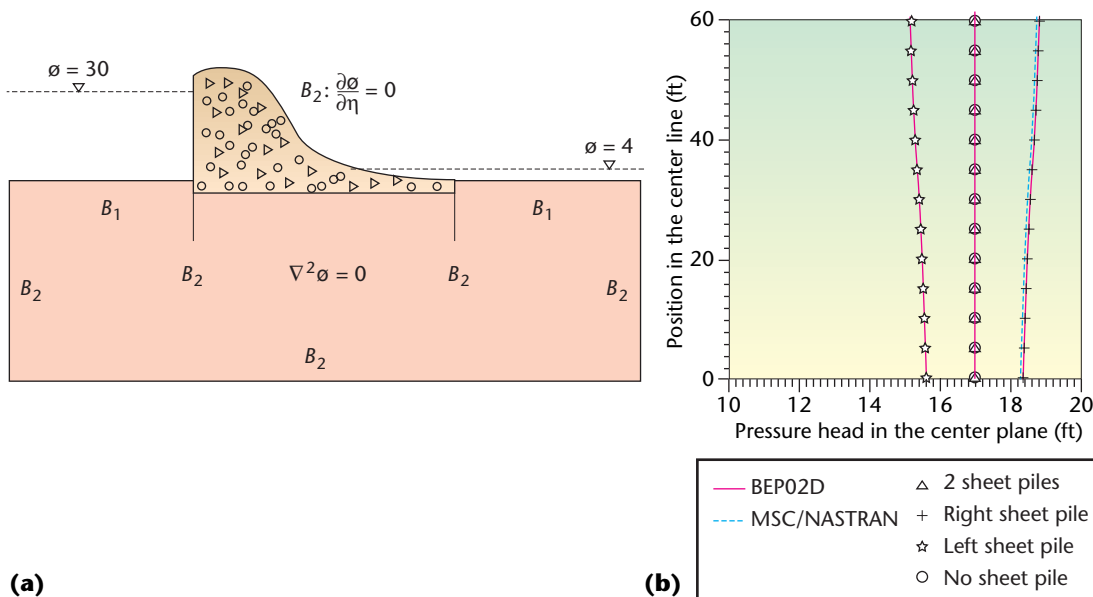


Figure 6. (a) A classical problem of seepage flow with sheet piles under a dam; (b) the pressure on the center plane under the dam.

symmetric, the flux distribution on both sides of the strip conductor is continuous. Therefore, we can obtain similar results to those listed in Table 2 from the conventional BEM, but the process of simulation is much different.

Consider a boundary  $B$  containing two parts: the nondegenerate boundary  $S$  and the degenerate boundary  $C^+$  and  $C^-$  as in Figure 5. For the DBEM, we can calculate a closed contour formed by two lines  $C^+$  and  $C^-$  (see Figure 5) for the degenerate boundary and the electric potential in just one run. For the conventional BEM, we can only model the nondegenerate bound-

ary, and we have to calculate the electric potential in two runs to avoid the degenerate boundary's effect. For some electrostatic problems without symmetric boundary condition, we could use just the DBEM, but we would need a subdomain technique with artificial boundaries in the conventional BEM.

From the results of the electric potential shown in Figure 4 and Table 2, we find that

- the conventional BEM without artificial boundaries cannot solve the electrostatic problem with degenerate boundary;

- the DBEM can analyze the electrostatic problem with degenerate boundaries efficiently;
- for the DBEM, the first set of kernels  $U(s,x)$  and  $T(s,x)$  must be used simultaneously with the second set,  $L(s,x)$  and  $M(s,x)$ ; and
- the differences between the FEM and DBEM are smaller than 4.3 percent.

Besides electrostatic problems, the DBEM is easily applicable to other areas with similar singular problems. Jeng-Tzong Chen, Hong-Ki Hong, and Shiang-Woei Chyuan, for example, have used dual integral formulation to deal with seepage problems.<sup>7</sup> In civil engineering, sheet piles or cut-off walls often occur because of flow problems through porous media (see Figure 6). The singular behavior in such an example is often ignored in numerical methods, with the expectation that the error will be limited to the singularity's vicinity. However, the formulation used must be capable of describing the singular behavior when the singularity arises from a degenerate boundary—for example, in seepage problems in which the singularity dominates the force exerted on the sheet piles. Using the DBEM, Chen, Hong, and Chyuan simulated four design cases of flow under a dam (see Figure 6a).<sup>7</sup> The results of pressure on the center plane under the dam between the DBEM and the FEM<sup>8</sup> were almost the same (see Figure 6b).

In addition to civil engineering, Chen and Hong also successfully applied the DBEM in the field of mechanical engineering.<sup>9</sup> For the thermal problem of heat conduction with singularity from degenerate boundary, the DBEM is particularly suitable for the singular problem of extremely localized and concentrated heat flux.<sup>9</sup>

To develop kernel functions of the DBEM in the future, researchers can extend the application from the Laplace equation of electrostatic problems to the Helmholtz equation of the electromagnetic wave.

## References

1. J.T. Chen and H.-K. Hong, "Review of Dual Boundary Element Methods with Emphasis on Hypersingular Integrals and Divergent Series," *Trans. ASME*, vol. 52, no. 1, 1999, pp. 17–33.
2. M.N.O. Sadiku, *Numerical Techniques in Electromagnetics*, CRC Press, 1992.
3. S. Chakravorti and H. Steinbigler, "Boundary Element Studies on Insulator Shape and Electric Field around HV Insulators with or without Pollution," *IEEE Trans. Dielectrics and Electrical Insulation*, vol. 7, no. 2, 2000, pp. 167–176.
4. H.-K. Hong and J.T. Chen, "Derivation of Integral Equations in Elasticity," *J. Eng. Mechanical Division*, vol. 114, no. 6, 1988, pp. 1028–1044.
5. A. Portela, M.H. Aliabadi, and D.P. Rooke, "The Dual Boundary Element Method: Effective Implementation for Crack Problems," *Int'l J. Numerical Methods Eng.*, vol. 33, 1992, pp. 1267–1287.
6. D.K. Cheng, *Field and Wave Electromagnetics*, Addison-Wesley, 1989.
7. J.T. Chen, H.-K. Hong, and S.W. Chyuan, "Boundary Element Analysis and Design in Seepage Problems Using Dual Integral Formulation," *Finite Elements in Analysis and Design*, vol. 17, 1994, pp. 1–20.
8. J.T. Chen et al., *Finite Element Analysis and Engineering Applications Using MSC/NASTRAN*, Northern Gate Publications, 1996 (in Chinese).
9. J.T. Chen and H.-K. Hong, "Application of Integral Equations with Superstrong Singularity to Steady State Heat Conduction," *Thermochimica Acta*, vol. 135, 1988, pp. 133–138.

**Shiang-Woei Chyuan** is working toward a doctoral degree in the Department of Mechanical Engineering at the National Taiwan University, Taipei, Taiwan, R.O.C. His technical interests include MEMS simulation and design, numerical modeling and simulation of electrostatics and electromagnetics, and aging life analysis of solid-propellant grains. He received his BS in naval architecture and marine engineering and his MS in aeronautical and astronautical engineering, from National Cheng Kung University. Contact him at the Chung Shan Inst. of Science and Technology, PO Box 90008-15-3, Lung-Tan, Tao Yuan 325, Taiwan, ROC; yeaing@iris.seed.net.tw.

**Yunn-Shiuan Liao** is a professor and director of traditional and nontraditional machining in the Department of Mechanical Engineering at National Taiwan University. His research interests include nontraditional machining processes, the machining of difficult-to-cut materials, and precision machining. He received his MS and PhD in mechanical engineering from the University of Wisconsin-Madison. He is a member of the ASME. Contact him at liaoyo@ccms.ntu.edu.tw.

**Jeng-Tzong Chen** is a professor in the Department of Harbor and River Engineering National Taiwan Ocean University. His technical interests include computational mechanics, the boundary element method, and vibration and acoustics. He received a BS in civil engineering, an MS in applied mechanics, and a PhD in civil engineering from National Taiwan University. Contact him at jtchen@mail.ntou.edu.tw.